Multidisciplinary Journal for Applied Research in Engineering and Technology (MJARET)

Vol. 1 Issue 4, November – 2021, Pages: 14-17

Calculation of Gabor Channel Surface Recovery Using Parameters

Sivakumar R
Assistant Professor, Department of ECE, PERI Institute of Technology
Chennai, India.
Email: apecproject4204@gmail.com

Abstract: For picture recovery, Gabor channels are often employed to extract surface highlights from images. The Gabor filter makes use of a variety of different factors (such as the number of scales and introductions and the measurement of channel cover). These criteria seem to have been chosen without enough explanations in the work that has been presented to yet. This work studies the implications of different Gabor channel parameters on surface recovery.

Keywords— Gabor channels, *Gabor Filter, channel parameters*

1. INTRODUCTION

A picture's surface is an essential component. Recent developments in surface research have made multichannel Gabor disintegration a popular choice. To separate surface highlights from images for either surface division [3, 4, 5] or picture recovery [6, 7, 8], the Gabor channel mimics the appearance of primary visual cortex cells in the brain [1, 2]. For example, Ma and Manjunath [7, 8] have shown that Gabor highlights outperform PWT, TWT, and MRSAR highlights when it comes to recovering images. In addition, the MPEG-7 surface description [9] acknowledges their commitment. The Gabor filter makes use of several different parameters. However, in the work that has been released thus far, these criteria seem to have been selected without enough explication. In Perona [10], the number of scales and introductions used in a variety of frameworks is recorded. Scales range from 4 to 11 and introductions range from 2 to 18 numbers. In addition, no research has been done on the optimum technique to pick channel veil measure. Until now. There are several Gabor channel characteristics that affect surface recovery that we investigate in this work. In practice, the viability and proficiency of surface recovery may be adjusted by varying the number of channels and the size of the channel veil.

One kind of joint inflammation that may result in ligament damage and breakdown is Osteoarthritis, and it affects at least one knee. Cartilage is the protein material that acts as a cushion between the bones of a joint. Osteoarthritis is the most common joint condition among the 100 different types of joint inflammation [1]. Many adults are affected by it, although it is a disease that is often misunderstood [2]. Approximately 80% of the population over the age of 65 has radiographic evidence of OA [3]. Over 16% of adults 45 years and older were found to have symptoms of osteoarthritis (OA) of the knee [4]. There is a noticeable, pathologic portion of articular ligament misery [5–6]. Articular ligament and meniscus damage, synovial inflammation and osteophytes are common causes of joint pain in patients. Swelling, anguish, pain, annoyance, locking, and other troubles with flexibility are among the symptoms [3]. Clinical pathology and medicine rely heavily on quick conclusions [7, 8].

Clinical and logical technologies to reliably assess the severity of knee OA are needed because of the high prevalence of OA. The "highest quality level" radiography (X-beam) is often preferred and remains the major accessible device for preliminary identification of knee OA, despite the introduction of a few imaging modalities, for example, MRI, Optical Coherence Tomography and ultrasound for larger OA investigation. Deterioration of joint ligaments reduced joint space between bones, and formation of bone goads are all common OA X-ray findings [13].

The severity of knee OA has previously been evaluated as a picture grouping problem [8, 10, 12]. As a first step, the picture modifications and content descriptors that are useful for picture examination are spotted in the X-beam images. It is via the use of X-beam images that the OA seriousness inquiry may be examined. Knee joint localization, as well as other uses like bosom mass detection [15], are all possible using x-beam images.

The current state of the Gabor filter

The purpose of a component extractor is to provide visual samples that may be used to improve the accuracy of a classification algorithm. Using a band-pass channel, such as Gabor, you may distinguish between different samples of a flag or piece of data at different frequencies. Gaussian dispersion is used to balance symphonious capabilities in the Gabor channel. Dennis Gabor first proposed the concept of a Gabor channel in the 1940s, and it wasn't until Daugman expanded on it in the 1980s that it was brought to 2D channels. The Gabor channel exhibits sinusoidal wave duplication with Gaussian capability. The authentic and imaginative elements are created separately by the Cosine and Sine waves.

One of Gabor's most well-known surface descriptors, the "Gabor channel," was first used in 1946. By dividing the image's recurrence space, it's linked to other distinct highlights. The Gabor channel is a complicated sinusoidal recurrence and introduction-tweaked Gaussian channel. Any number of measurements may be performed in both spatial and recurrence space. Due to their superior surface fineness, these channels are more appealing. Examining the Gabor channel involves doing an IFFT on the results of performing a Fourier change on the image and then raising the Gaussian capacity focused on various frequencies. The choice of each Gaussian's focused recurrence is crucial in ensuring that all of the picture's frequencies are protected.

The complex Gabor filter may be defined as the product of the complex sinusoid product with the Gaussian kernel times. Gabor filters are effective band-pass filters for single-dimensional signals such as speech, ECG, and so on. What the public is doing:

$g(t) = kej\theta\ w(at)s(t)$

Here, $w(t) = e^{-\pi t2}$

$s(t) = e^{j(2\pi fot)}$

$e^{j\theta}s(t)e^{j(2\pi fot+\theta)} = (\sin(2\pi fot + \theta), j\cos(2\pi f_o t + \theta))$

Here k, θ, f_o are filter parameters.

Here k, θ, fo are filter parameters.

Complex version of Gabor filter is determined as two phase filters are allocated continuously in the real and complex part of a filter function,

The real part have the filter

$gr(t) = w(t)\sin(2\pi fot + \theta)$

The imaginary part have the imaginary filter function

$gi(t) = w(t)\cos(2\pi fot + \theta)$

Proposed Gobar Filter Extensions:

As a way to achieve the Gabor highlights, photos must be conjoined with each of the channels. In addition, the convolution takes a long time because of the large image size and the computational many-sided quality of the convolution. Convolution operations in spatial areas may be replaced by increases in recurrence space for speedy speed in large images. The source image and the Gabor channels must be transformed using FFT and IFFT, respectively, before the convolution process can begin. FFT and IFFT's temporal complexity is O(S2 log2 S), where S * S denotes the image size. Time unpredictability is projected to increase with each extra pixel in the channel veil measure (the set of channel coefficients). More Gabor Filters also necessitates a bigger amount of storage space and complexity in the storing of the coefficients as well as the component vectors. As a result, the selection of parameters is critical. According to our calculations, our findings are sound.

It is necessary to describe the channels using a bank of Gabor filters in order to carry out surface recovery. As the wavelet transform's wavelet function, the Gabor function is assumed to be the filter set's relative basis. The filtered pictures are used to recreate the input image using a systematic filter selection technique. A bounded nonlinear transformation is applied to the filtered picture, and this serves as a texture detector. To create a multi-level surface, the filtering and nonlinear stages are combined. The distinctions in the characteristics of the various areas aid in texture discrimination.

The Gabor filter extension equation is

$$h(x,y) = \exp\left\{-\frac{1}{2}\left[\frac{x^2}{\sigma_x^2} + \frac{y^2}{\sigma_v^2}\right]\right\}\cos(2\pi u_0 x + \phi)$$

The 2-D Gabor filter function, referred to as such because it needs values in both the spatial and spatial-frequency domains, is required for surface recovery. It is preferable to utilise filters with low bandwidth in the spatial-frequency domain because they can distinguish between various surfaces. Alternatively, precise localization of surface boundaries necessitates the use of spatially-localized filters. The inverse relationship exists between the spatial-frequency domain bandwidth and the spatial-domain effective breadth of a filter. Optimal joint localization, or resolution, in both the spatial and spatial-frequency domains, is a

Multidisciplinary Journal for Applied Research in Engineering and Technology (MJARET)

Vol. 1 Issue 4, November – 2021, Pages: 14-17

key characteristic of Gabor filters.

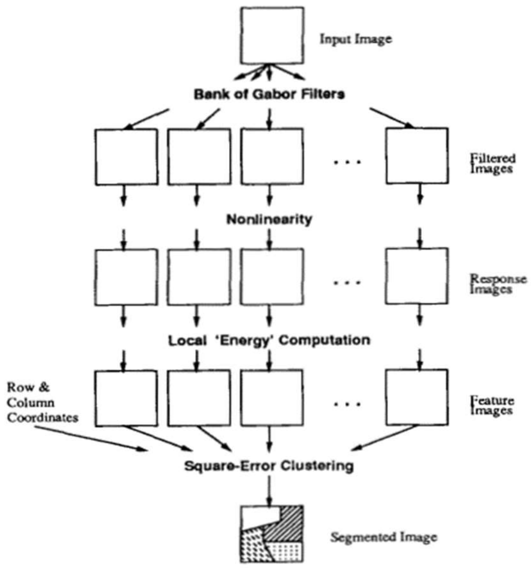

As per literature, 2-D Gabor function does not have a standard expression yet, its core idea is Gaussian function modulated by complex sine function

$$g(x,y)=\frac{1}{2\pi\sigma_x\sigma_y}\exp\left[\frac{-x^2}{2\sigma_x^2}+\frac{-y^2}{2\sigma_y^2}\right]\times\exp[jw(x\cos\theta+y\sin\theta)]$$

$$g_e(x,y)=\frac{1}{2\pi\sigma_x\sigma_y}\exp\left[\frac{-x^2}{2\sigma_x^2}+\frac{-y^2}{2\sigma_y^2}\right]\times\cos[w(x\cos\theta+y\sin\theta)]$$

$$g_o(x,y)=\frac{1}{2\pi\sigma_x\sigma_y}\exp\left[\frac{-x^2}{2\sigma_x^2}+\frac{-y^2}{2\sigma_y^2}\right]\times\sin[w(x\cos\theta+y\sin\theta)]$$

The responses are recorded for various Gabor filter functions are recorded as,

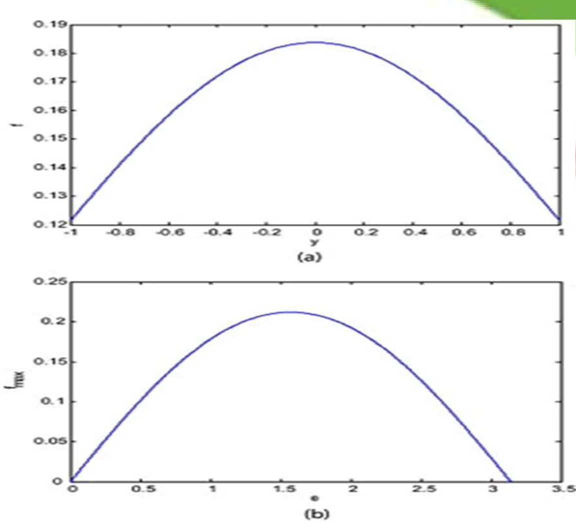

Fig 2: Influence of Spatial and Frequency domain parameters y and θ on the response. (a) f(y) with respect to y, (b) fmax with respect to θ

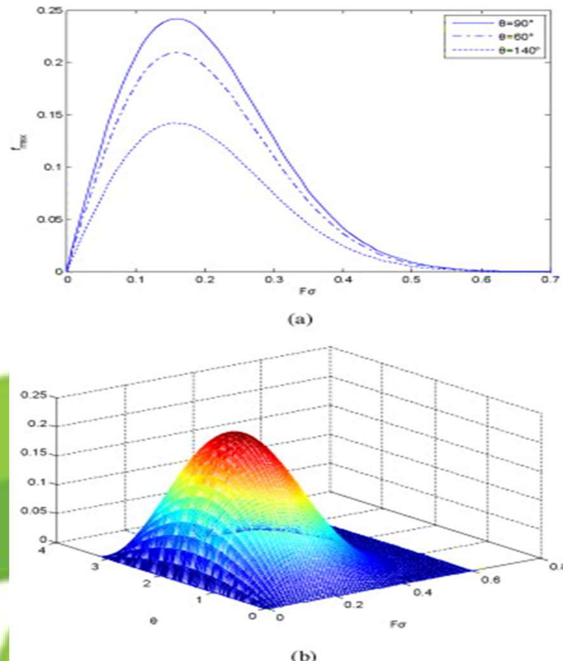

Fig 3: 2-D Gabor filter response on surface discovery using Spatial and Spatial - Frequency domain parameters fmax and f0. (a) f0 with respect to fmax, (b) f0 with respect to θ

CONCLUSION:

Gabor Filter is the current channel when the example isn't accurate and the response isn't suitable for OA analysis. As a result, a channel with a more precise design is in the works, and it will aid in the analysis of OA using human x-rays. As a result of using the Extended Gabor channel functions in conjunction with this image dataset, component vector estimation yielded better accuracy. By mapping an extended Gabor channel, complicated Gabor Filter functions may be used in both spatial and frequency domains. We'll be able to apply the arrangement calculation to the channel in the future since we've already defined the KL review.

REFERENCES

[1] Daugman, J.G., “Two-dimensional spectral analysis of cortical receptive field profiles,” Vision Research, Vol. 20, pp. 847-856, 1980.

[2] S. Marcelja, “Mathematical description of the responses of simple cortical cells,” J. Opt. Soc. Amer., vol. 70, no. 11, pp. 1297-1300, 1980.

[3] K. Jain and F. Farrokhnia, “Unsupervised texture segmentation using Gabor filters,” Pattern Recognition, Vol. 24 no. 12, pp. 1167-1186, 1991.

[4] Dunn, D. and Higgins, W.E., “Optimal Gabor filters for Texture Segmentation,” IEEE Transactions on Image Processing, Vol. 4, No. 7, pp. 947-964, Jul 1995.

[5] Dunn, D., Higgins, W.E. and Wakeley, J., “Texture segmentation using 2-D Gabor elementary functions,” IEEE Transactions on Pattern Analysis and Machine Intelligence, Vol. 16, No. 2, pp. 130-149, Feb. 1994.

[6] Dengsheng Zhang, Guojun Lu, “Content-based image retrieval using Gabor texture features”, In Proc. Of First IEEE Pacific- rim Conference on Multimedia (PCM”00), pp.1-9, Fargo, ND, USA, June 1-3, 2001.

[7] P. Wu, B.S.Manjunath, S.D. Newsam and H.D.Shin, "A Texture Descriptor for Image Retrieval and Browsing", Computer Vision and Pattern Recognition Workshop, Fort Collins, CO, USA, June 1999.

[8] B.S.Manjunath and W.Y. Ma, "Texture features for browsing and retrieval of image data", IEEE Transactions on Pattern Analysis and Machine Intelligence (PAMI), vol.18, no.8, pp.837-42, Aug 1996.

[9] B.S. Manjunath, Phillipe Salembier, Thomas Sikora, Introduction to MPEG-7 : multimedia content description interface, Chichester; Milton (Qld.) : Wiley, 2002.

[10] Perona, P., “Deformable kernels for early vision,” IEEE Transactions on Pattern Analysis and Machine Intelligence, Volume: 17, Issue: 5, pp. 488-499, May 1995.